Electronic Supplementary Material (ESI) for Physical Chemistry Chemical Physics

SUPPLEMENTAL INFORMATION

pH changes the aggregation propensity of Amyloid-β without altering the monomer conformation

*Debanjan Bhowmik[1], Christina M. MacLaughlin[2], Muralidharan Chandrakesan[3], Prashanth Ramesh[1], Ravindra Venkatramani[1], Gilbert C. Walker[2] and Sudipta Maiti[1]**

[1]Department of Chemistry, Tata Institute of Fundamental Research, Homi Bhabha Road, Colaba, Mumbai 400005, India.

[2]Department of Chemistry, Lash Miller Laboratories, University of Toronto, Toronto, ON M5S 3H6, Canada.

[3]Department of Biochemistry, Seth G.S. Medical College and KEM Hospital, A.D. Marg, Parel, Mumbai 400012, India.

Corresponding author: *Email: maiti@tifr.res.in

Materials and Methods:

Silver Nanoparticle Synthesis: 1 mM 50 ml $AgNO_3$ solution was taken in a 500 ml round-bottom flask and heated to boil. 0.114 g of trisodium citrate dihydrate was dissolved in 10 ml of water. As soon as the silver nitrate solution started boiling 1 ml of the trisodiumcitrate solution was added to it. The solution was refluxed for 1 hr and then cooled to obtain the nanoparticle solution. $AgNO_3$ was purchased from Merck (Schuchardt, Germany) and trisodium citrate was purchased from Sigma-Aldrich Inc. (St. Louis, MO, USA).

Characterizations of Ag nanoparticles: The surface plasmon resonance of the synthesized silver nanoparticles was characterized by absorption spectroscopy. Absorption spectra of the synthesized nanoparticle solutions (Fig. S1A) are recorded in a JASCO spectro-photometer, after diluting the solution ten-fold by water. The absorption maximum was found to be at 410 nm (Figure S1A), which should correspond to an average spherical particle diameter of ~40 nm. However, a small shoulder observed at a shorter wavelength (~350 nm) was possibly due to higher order multipoles, and indicated the presence of a small amount of bigger and/or non-spherical particles. We do note that the quadrapoles in some cases may be optically dark but still provide strong local field enhancements of Raman scattering (Z. Fakhraai, personal communication.). The size distribution of the nanoparticles (Fig. S1B & S1C) is examined with a transmission electron microscope (LIBRA 120, EFTEM, Carl Zeiss, Germany). One of the representative TEM images of silver nanoparticles is shown in Figure S1B. Analysis of eight such fields containing >100 particles shows that >85 % of the particles are spherical. The distribution of particle diameter (considering only spherical particles) is shown in Figure S1C. Most of the spherical particles had diameters in the range of 30-60 nm, as shown.

Surface Modification of Ag-nanoparticles: To prepare particles for the SERS measurements, 2 ml of the nanoparticle solution was centrifuged at 16,000 g for 30 mins. The supernatant was discarded followed by resuspension of the nanoparticles in 100 μL of dialyzed monomeric cys-Aβ solution. As a control, 100 μL dialyzed buffer not containing any peptide was also added in a separate sample after centrifugation. The resuspended solutions were kept rotating for 10 mins. The desired pHs always were obtained by adding 5mM phosphate buffer (pre-adjusted to different pHs) before the SERS measurements. Raman spectra were recorded with a Confocal Raman Microscope (Witec alpha300 RS, Germany) by exciting at 514 nm using 200-300 μW power and 10 min of integration time. A 50X, 0.55 NA Zeiss air objective was used and the emission was collected by a 100 μm diameter optical fiber in a confocal geometry.

Zeta potential measurement: The samples prepared for SERS experiments were also subjected to zeta potential measurement after 5 fold dilution with water. The measurements are performed with a ZetaPALS – Zeta Potential Analyser (Brookhaven Instruments Corporation, USA). Each reported average values are results of 10 cycles of measurement.

Citrate capped particles had a zeta potential value of -37.4±1.2 mV, and $A\beta_{40}$-Cys capped particles had a zeta potential value of -37.3±3.6 mV. This indicates that the particles are reasonably stable, and that the stability is not hampered by surface functionalization.

Peptide synthesis and fluorophore labeling: C- terminal cysteine containing $A\beta_{40}$ ($A\beta_{40}$-Cys) and N-terminal rhodamine labeled $A\beta_{40}$-Cys ($RA\beta_{40}$-Cys) were synthesized, purified and characterized in the laboratory. The peptides were synthesized using 9-fluorenylmethoxycarbonyl (Fmoc) chemistry in an automated solid phase peptide synthesizer (PS3, Protein Technologies Inc. Tucson, AZ, USA). N-terminal Rhodamine labeling to $A\beta_{40}$-Cys was performed on solid support. In brief, the free amino terminal of the peptide was treated with

a mixture of 5(6) Carboxy Rhodamine N-Succinimidyl ester (4 fold mole excess), 1-hydroxybenzotriazole (HOBT, 2 fold excess) and collidine (4 fold excess) in N,N-dimethylformamide (DMF). The coupling was extended for 7 days and the resin was washed with DMF, Methanol till no fluorescence was detected in the wash. The peptide was cleaved, purified and mass checked following protocols describe elsewhere.[1] 5(6) Carboxy Rhodamine N-Succinimidyl ester was purchased from Merck (Schuchardt, Germany). HOBT, collidine, methanol and DMF were purchased from S.D. Fine Chem. Ltd. (Mumbai, India).

Preparation and characterization of Monomers: We have earlier found that at very low concentrations, monomers of $A\beta_{40}$ are the only thermodynamically stable species at physiological conditions. Monomers can be obtained spontaneously from oligomeric mixtures upon long term incubation in physiological buffer solutions[2] and this is the method we used here for preparing the monomers.

A stock solution of 1 mM $A\beta_{40}$-Cys was prepared at pH 11 aqueous NaOH solution. A separate stock solution of 333 μM of $A\beta_{40}$-Cys and 10 μM of N-terminal rhodamine B labeled $A\beta_{40}$-Cys ($RA\beta_{40}$-Cys) was also prepared. The stock solutions were then diluted to give 1 μM of peptide in aqueous buffer (consisting of 20mM Na_2HPO_4, 150 mM NaCl, 5.4 mM KCl, 2mM NaN_3; pH adjusted to 7.4). The size of the peptide in the solution was monitored by Fluorescence Correlation Spectroscopy (FCS) as a function of incubation time for three weeks (using the fluorescence from trace amounts of $RA\beta_{40}$-Cys present in the solution). The hydrodynamic radius of the peptide decreased over this period of time from 1.6 nm to 0.9 nm, due to the formation of monomers from small oligomers (figure S2). Previous experiments from our lab have established the hydrodynamic radius of monomer of Rhodamine B labeled $A\beta_{40}$ to be 0.9 nm.[2]

The solution without the rhodamine B labeled $A\beta_{40}$-Cys (also incubated for three weeks in similar condition as that of the solution containg the $RA\beta_{40}$-Cys) was then used for the SERS experiments.

Molecular Dynamics simulations:

Model system: Our model system for simulation was derived from the $A\beta_{40}$ monomer structure from NMR studies in aqueous micellular environments (PDB id: 1BA4). The 1BA4 NMR secondary structure shows α helical character in the region between residues 15-38 whereas the remaining regions adopt a random coil conformation (Fig S3). The rational for choosing this structure is as follows. The SERS experiments report significant α-helical character in the monomer solution structure. Previous simulation studies over long timescales have shown that the monomer adopts a variety of conformations in water including helices, sheets, and random coils.[3] We can thus readily test our questions of interest: the ability of electric fields to stabilize/destabilize the helical region and/or to introduce a helix in unstructured peptide regions, by comparing structures of $A\beta_{40}$ in water (derived from molecular dynamics simulations of similar timescales) in the presence/absence of electric fields. Since the experiments were performed on $A\beta_{40}$ peptides with a cysteine linker, we modified the 1BA4 structure by modeling a cysteine residue at the C-terminus to create a $A\beta_{40}$–Cys system (Fig S3) for the simulations.

Simulation protocol: All the simulations were performed using the NAMD simulation package.[4] System preparation, visualization of simulation trajectories, and data analysis were carried out using the VMD software.[5] The initial coordinates of the Aβ monomer were obtained from an NMR structure of $A\beta_{40}$ monomer (structure 4 from PDB ID: 1BA4) in aqueous sodium dodecyl sulfate (SDS) micelles. The justification for using the 1BA4 structure

was presented in the preceding paragraph. The 1BA4 structure was modified using the software package Modeller (http://salilab.org/modeller/) to include a cysteine residue at the C-terminus to create the $A\beta_{40}$-Cys model in Fig S3. The protonation states of the sidechains and termini were modified to simulate the behaviour at pH 7 (positively charged N-terminus, lysines and arginines, negatively charged C terminus, aspartates and glutamates and neutral histidines). The CHARMM27 force field was used.[6] The protein was then immersed in an 8.6nm X 8.6nm X 8.6nm water box and neutralized with Na^+ counter ions. The system was first subjected to an energy minimization. Subsequently a heating and equilibration step was carried out, which involved the steady increment of temperature in steps of 6K/1ps from 0K to 300K followed by an equilibration at 300K for 50ps. This protocol was initially followed with the protein fixed (free hydrogen bond angles and torsions) and then with harmonic constraints (25 kcal/mol/$Å^2$) on the protein heavy atoms. This was followed by an NPT (constant pressure and temperature) equilibration run for 1ns at 300K to stabilize the density of the system at a pressure of 1 atm. During the NPT run the harmonic constraints on the protein heavy atoms were gradually released and the solvation box dimensions relaxed to 8.3nm X 8.3nm X 8.3nm. A 100ps NVT (constant volume and temperature) equilibration at 300K followed this, giving an equilibrated and stabilized $A\beta_{40}$-Cys system consisting of the solvated polypeptide. All subsequent NVT production runs (with and without electric fields) were performed starting from the same structure obtained at the end of the NVT equilibration run. All simulations employed periodic boundary conditions with the Particle Mesh Ewald (PME) algorithm describing long range electrostatics. The van der Waals forces were calculated with the use of a switching function that has 10Å as switching distance and 12Å as cutoff.

We carried out two 5ns NVT control simulations at 300 K (termed FREE-1 and FREE-2) in the absence of electric fields to assess the structural stability and dynamical relaxation of $A\beta_{40}$–Cys peptide in solution. Any structural relaxations induced by external electric fields were to be determined by comparing/contrasting simulations in the presence of electric fields with the FREE controls. Two 5ns simulations (TEMP-EF-1 and TEMP-EF-2) of the $A\beta_{40}$ –Cys system in the presence of electric fields were carried out by applying uniform charge dependant forces on the atoms of the system during the simulation. We implemented scripts to numerically describe the temporally varying electric fields within the MD simulation framework of NAMD. The experimental setup assumed in our studies, consists of laser light of frequency 514nm incident on a circular area of diameter 560nm, and power of 200 – 300 μW. Accordingly we carried our simulations with temporally varying (labeled TEMP-EF) electric fields modeled by a square wave of period 2fs (corresponding to visible light frequency). This implies that the field reverses direction every time step (1 fs) of the simulation. This experimental setup assumed above generates an electric field of amplitude ~1 mV/nm. We estimated a surface plasmon enhancement factor of 100 in magnitude i.e enhanced electric field strength of 0.1V/nm. The magnitude of the electric field was chosen to be 1V/nm, which is an order of magnitude larger than the estimated surface plasmon field in order to compensate for the short (nanosecond) time scales of our simulation. Simulations of proteins using a static electric field of similar strengths as the temporal electric fields applied here (unpublished data), showed that the strong static electric field induces major conformational changes within several hundreds of picoseconds. Thus, the order of magnitude longer (5ns) simulations used in this study are sufficient to assess the effect of the temporal electric field on the structure and dynamics of the $A\beta_{40}$–Cys peptide in solution.

All the different control and electric field production simulations were carried out for 5ns at a temperature of 300K. The different molecular dynamics simulation trajectories were consolidated to obtain snapshots representing the coordinates of the $A\beta_{40}$–Cys peptide and solvent molecules at every 1000^{th} time step (every 1 picosecond) of the simulation.

Structural changes observed in simulations: Figure S4A shows the initial and final structures obtained from the FREE-1, FREE-2, TEMP-EF-1, and TEMP-EF-2 simulations. Pande and co-workers have recently shown using long timescale simulations that the Aβ monomers are intrinsically disordered in solution accessing a wide range of isoenergetic conformations with some α-helical propensity.[3] Our starting $A\beta_{40}$-Cys structure derived from NMR studies is thus expected to lose its strongly α-helical character in water. As seen in the Fig S4A, our simulation timescales are too short to capture such conformation transitions, and the helix in the region 15-38 was found to be stable over the 5ns timescale in both FREE-1 and FREE-2 simulations. In agreement with these control simulations, the TEMP-EF structure at 5ns also shows a highly stable helix formed by residues 15-38 and the only structural changes appear to be in the unstructured random coil regions of the peptide.

In order to asses any effect of the temporally varying electric field on the dynamics of peptide, the Root Mean Square Deviation (RMSD) of the peptide structure from the initial NVT equilibrated $A\beta_{40}$–Cys structure used for the production trajectories of TEMP-EF and FREE simulations were compared. Since no fixed reference frame for alignment exists for the unstructured random coil regions of the peptide, the RMSD alignments were performed using the helical segment between residues 15-38. As shown in Fig S4B, the RMSD of heavy atoms in the helical segment between residue 15-38 for the two TEMP-EF trajectories closely follows that for the two FREE trajectories. Overall, the plots in Fig S4B show that differences in RMSD

structural variations of the helical segment between the TEMP-EF and FREE simulations match those between the two FREE control simulations. No discernible effect of the temporally oscillating field on time evolution of the helical region is observed when compared to that in the free simulations over the 5ns trajectory.

These results described in the preceding paragraph show that even intense fields (about two orders of magnitude higher in intensity than those applied in our experiments) do not perturb either the structure or dynamics of the $A\beta_{40}$–Cys peptide in solution. Thus, the helical character of the Aβ monomers observed in our SERS experiments are likely physiological and not induced by the intense electric fields in the vicinity of the Ag nanoparticles. We hypothesize that the high frequency field reversals (on a 1 fs timescale) cannot couple to conformational changes in the protein which happen on a much slower (100s of femtoseconds to picoseconds) timescale. Thus visible light plasmon based spectroscopic techniques might be well suited for probing biomolecular structure and dynamics in low concentration solutions.

References:

1. V. S. Mithu, B. Sarkar, D. Bhowmik, M. Chandrakesan, S. Maiti and P. K. Madhu, *Biophys J*, 2011, **101**, 2825-2832.
2. S. Nag, B. Sarkar, A. Bandyopadhyay, B. Sahoo, V. K. Sreenivasan, M. Kombrabail, C. Muralidharan and S. Maiti, *J Biol Chem*, 2011, **286**, 13827-13833.
3. Y. S. Lin, G. R. Bowman, K. A. Beauchamp and V. S. Pande, *Biophys J*, 2012, **102**, 315-324.
4. J. C. Phillips, R. Braun, W. Wang, J. Gumbart, E. Tajkhorshid, E. Villa, C. Chipot, R. D. Skeel, L. Kale and K. Schulten, *J Comput Chem*, 2005, **26**, 1781-1802.
5. W. Humphrey, A. Dalke and K. Schulten, *Journal of molecular graphics*, 1996, **14**, 33-38, 27-38.
6. A. D. MacKerell, D. Bashford, M. Bellott, R. L. Dunbrack, J. D. Evanseck, M. J. Field, S. Fischer, J. Gao, H. Guo, S. Ha, D. Joseph-McCarthy, L. Kuchnir, K. Kuczera, F. T. K. Lau, C. Mattos, S. Michnick, T. Ngo, D. T. Nguyen, B. Prodhom, W. E. Reiher, B. Roux, M. Schlenkrich, J. C. Smith, R. Stote, J. Straub, M. Watanabe, J. Wiorkiewicz-Kuczera, D. Yin and M. Karplus, *J Phys Chem B*, 1998, **102**, 3586-3616.

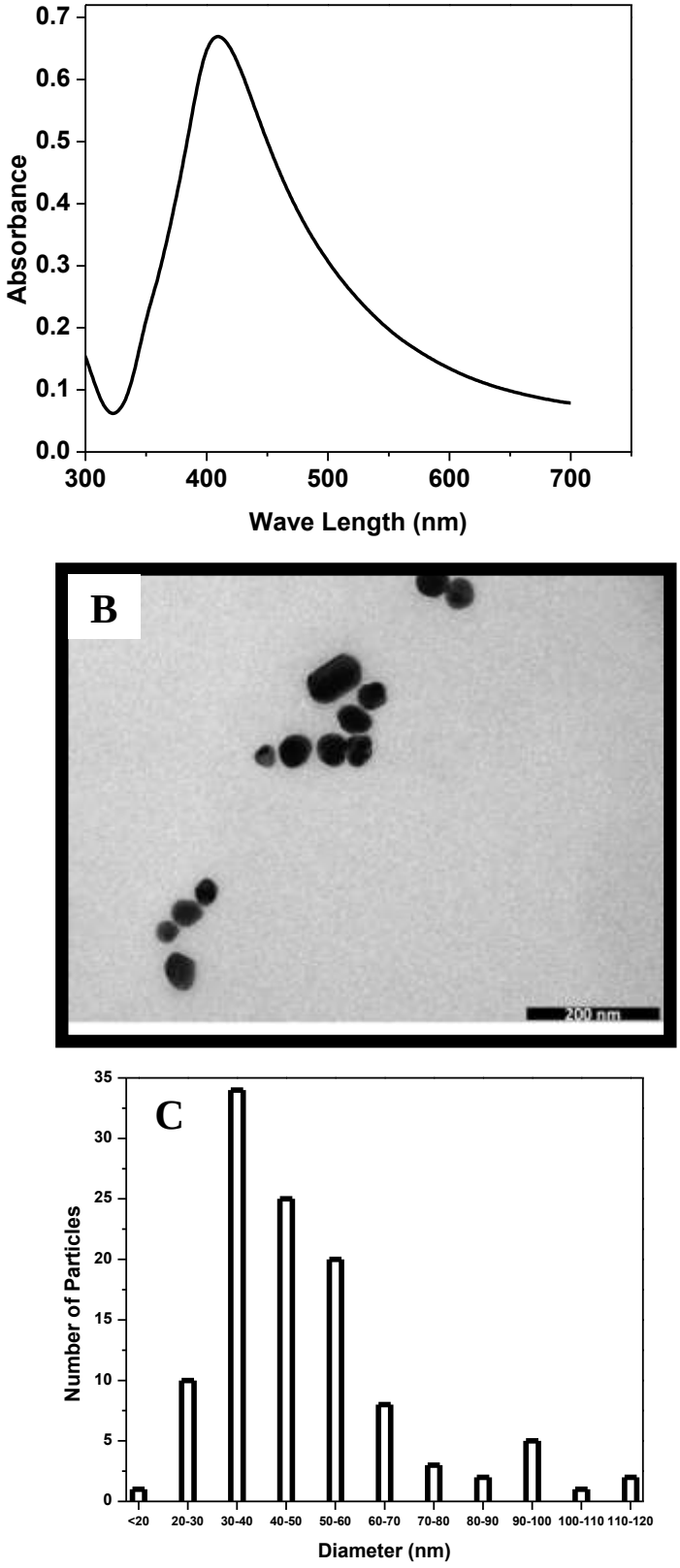

Figure S1: Characterization of silver nanoparticles. (A) Extinction spectra (having contribution from both actual absorbance and scattering) of synthesized Ag nanoparticles. (B) TEM image of Ag nanoparticles. (C) Particle size distribution obtained from the TEM image.

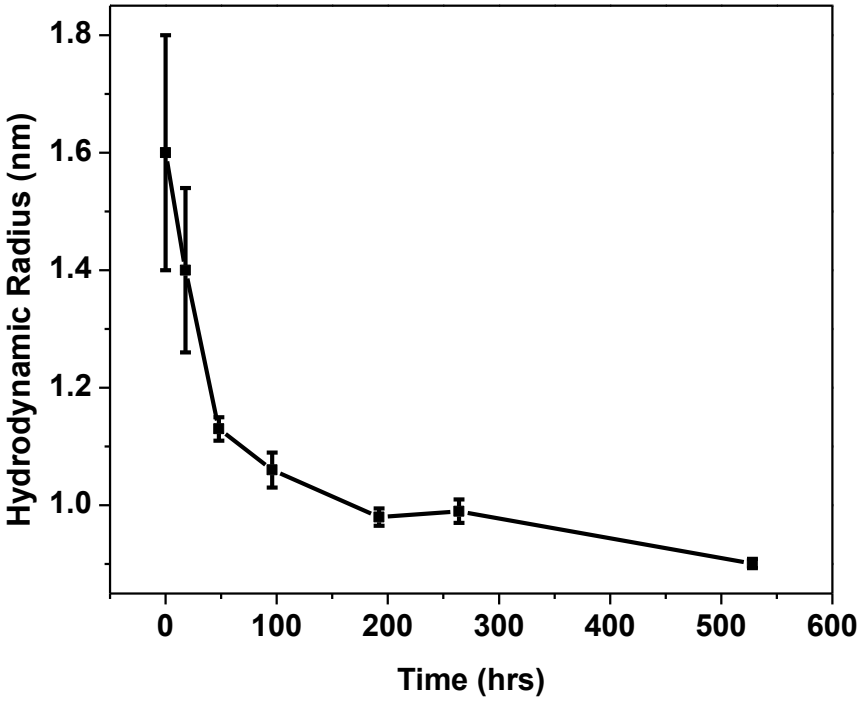

Figure S2: Hydrodynamic radius of rhodamine B labeled $A\beta_{40}$-Cys ($RA\beta_{40}$-Cys) as a function of incubation time, as measured by Fluorescence Correlation Spectroscopy.

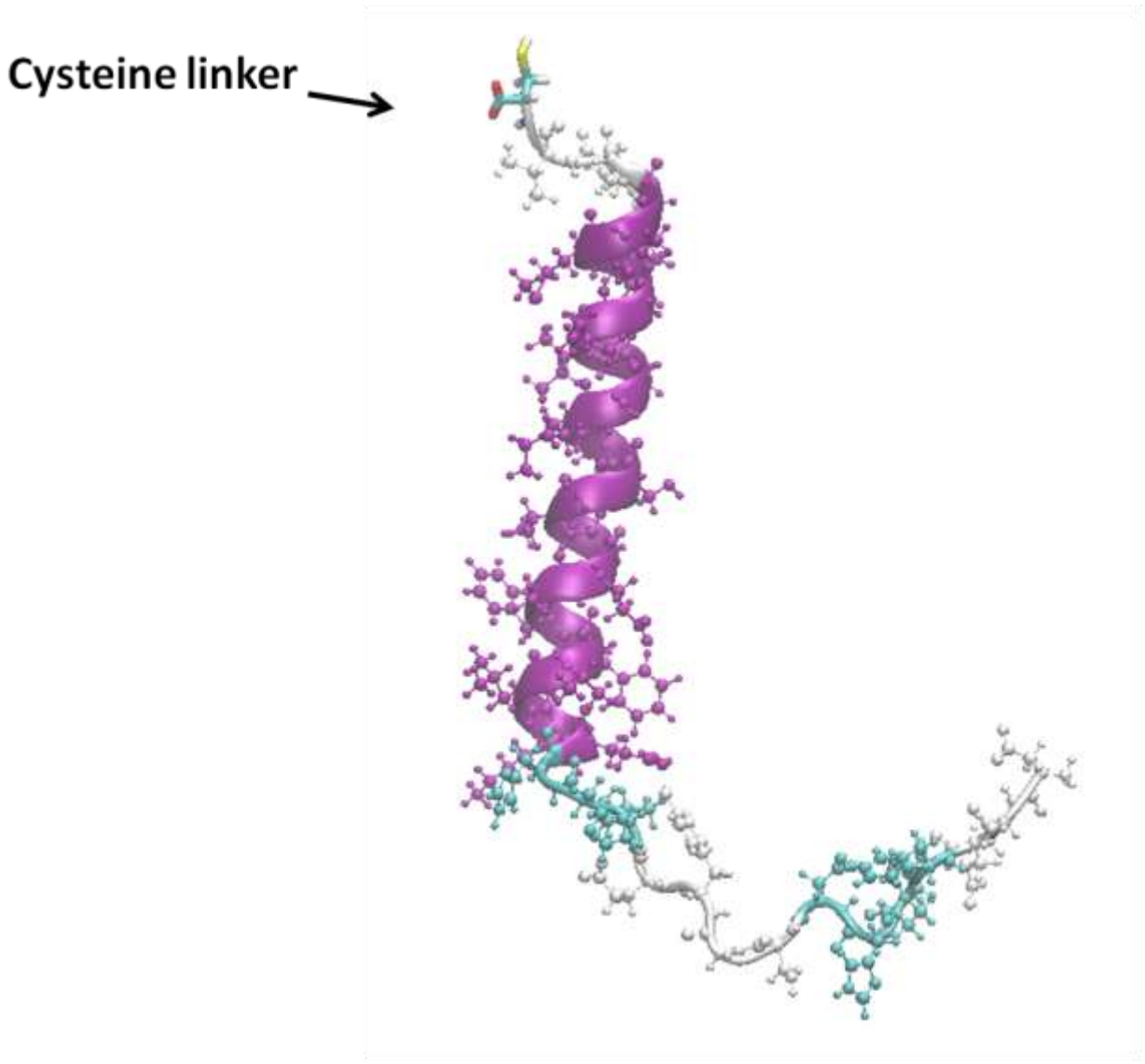

Figure S3: $A\beta_{40}$-Cys model with Cysteine linker (licorice representation) derived from NMR solution structure (PDB : 1BA4).

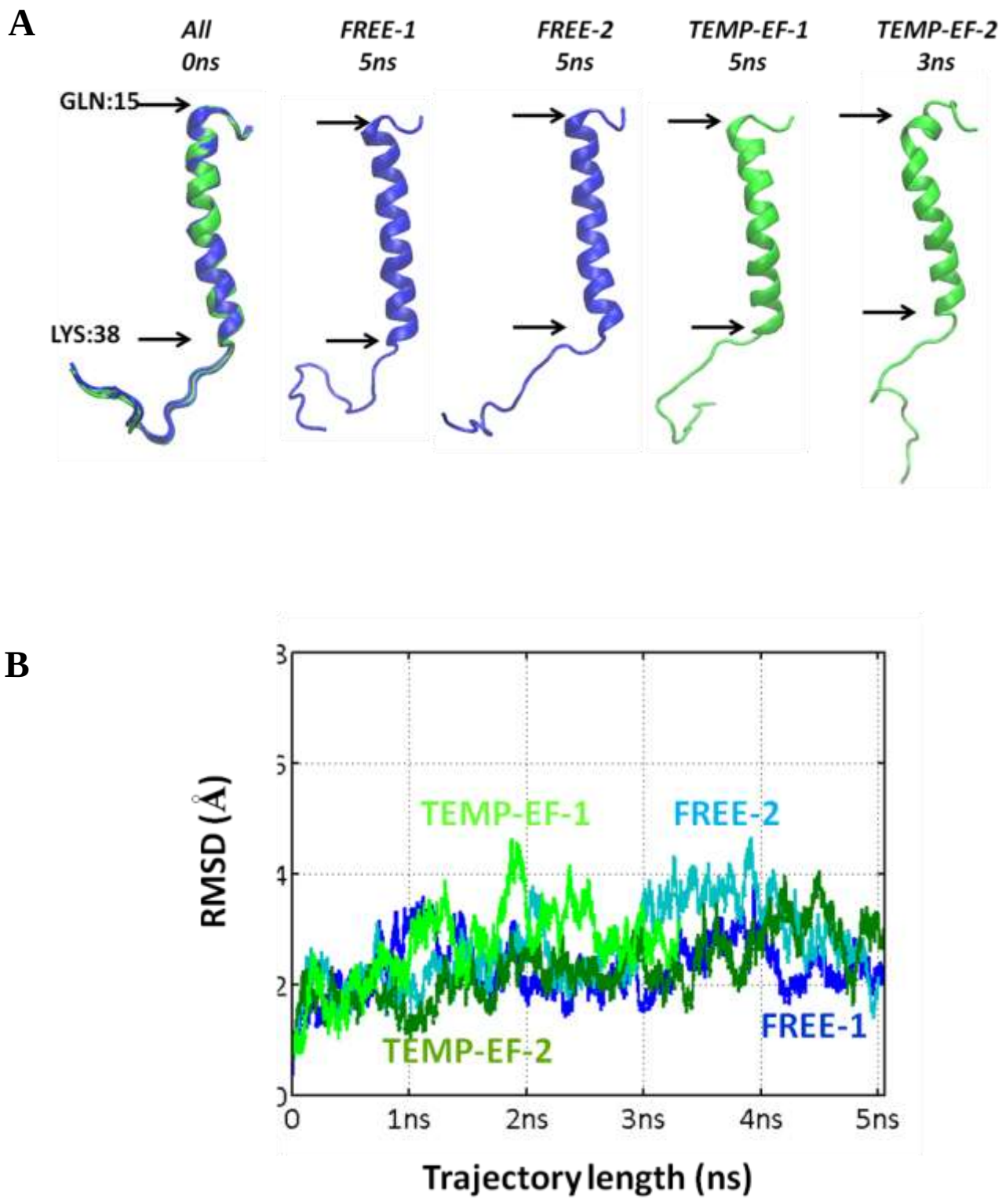

Figure S4: A) Backbone conformations of the $A\beta_{40}$-Cys monomer at the beginning and at the end of a 5ns molecular dynamics simulation trajectory. We compare two simulations with no electric fields at 300K (FREE-1 and FREE-2) and two simulations with a temporally varying electric

field (TEMP-EF-1 and TEMP-EF-2) reflecting the plasmon enhanced laser intensity present in the experiments in the vicinity of the nanoparticles.

B) Fluctuations in RMSD of heavy atoms in the helical segment (residues 15-38 shown in Fig S4A) of the $A\beta_{40}$-Cys peptide along the simulation trajectory recorded with respect to the structure at 0 ns.